RAPIDITY DISTRIBUTIONS OF LARGE TRANSVERSE MOMENTUM PARTICLES AND REALISTIC JETS

J. RANFT AND GISELA RANFT

Sektion Physik, Karl-Marx-Universität, Leipzig*

(Received September 7, 1976)

Cross sections and correlations of large transverse momentum particles are calculated in the hard collision model as function of the transverse momenta and of the rapidities. We choose jets with deviation from scaling and limited transverse momenta relative to the jet axis and find short range rapidity correlation of large transverse momentum particles on the same or the opposite side as the trigger particle. The correlation length is related to the width of the transverse momentum distribution in the jet system and decreases with rising transverse momenta of the two particles, quite in agreement with experimental data.

1. Introduction

There was considerable progress in the experimental exploration of collision processes with large transverse momentum particles within the last year [1, 2]. In this paper we use the hard collision model as in Ref. [3] (which in the following is denoted by I) for the calculation of inclusive cross sections for the production of one or several large transverse momentum particles. In I we studied the properties of jets and worked out large transverse momentum correlations at $\vartheta \simeq 90°$ as function of transverse momentum. The emphasis of the present paper is on correlations of large transverse momentum particles in the rapidity variable.

The hard collision model used here is the same as in I but in order to study the rapidity dependence of particle production cross sections we have to specify the angular dependence of the underlying jet production cross section. Throughout the paper we use a jet production cross section which corresponds to the irreducible subprocess parton + antiparton → jet + jet, but we concentrate mainly on the kinematics, on the properties of large transverse momentum particle production influenced by the properties of jets but not on the dynamics of jet production. For the purpose of our calculation we could have used also different dynamical jet production mechanisms.

* Address: Karl-Marx-Universität, Sektion Physik, 701 Leipzig, Linnéstrasse 5, GDR.

Our jets — introduced in I — deviate from scaling at finite energy and are characterized by limited transverse momentum of the particles relative to the jet axis. We stress that jets with total momenta below 2 GeV/c decay still rather isotropically; the unisotropic jet like nature develops rather slowly only at higher momenta. Large transverse momentum correlations are only known experimentally for trigger momenta of 2 to 3 GeV/c. Therefore, in order to compare with present experiments it seems to us that the non-asymptotic properties of jets are essential.

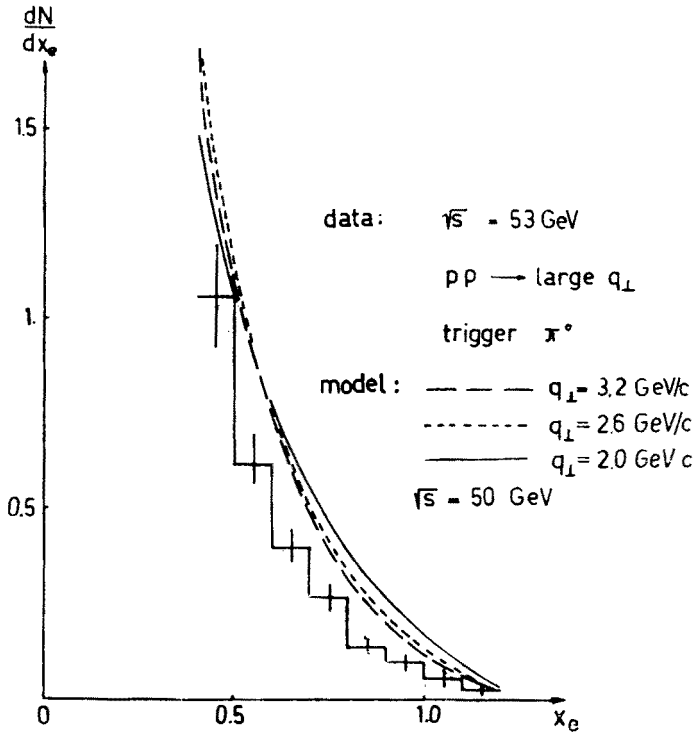

Fig. 1. Comparison of the opposite side distribution dN/dx_e according to Ref. [12] compared with curves due to our jet parametrization. It is $x_e = q_{\perp 2}/q_{\perp 1}$ where particle 1 is the same side trigger and $q_{\perp 2}$ is the transverse momentum of the opposite side particle

The model has been used successfully to describe same side large transverse momentum correlations [4, 3, 5] and opposite side large transverse momentum correlations [4, 5]. Our description differs from the one in Ref. [5] in two respects:

(*i*) In contrast to our treatment Ellis et al. use jets with exact scaling.

(*ii*) Ellis et al. find evidence for jets containing only one particle and describe them by a second delta-function like contribution to the inclusive jet fragmentation function. Conclusion (*ii*) was reached by Ellis et al. [5] from the comparison of the opposite side distribution dN/dx_e with data from Darriulat et al. [12]. We agree that it would be better to replace the inclusive jet fragmentation function by the sum of exclusive contributions from jets fragmenting into a definite number $n = 1, 2, \ldots$ of particles. As long as we do

not use such a description the inclusive jet fragmentation function is only expected to approximate the sum of these contributions.

In Fig. 1 we compare the same data on dN/dx_e [12] used by Ellis et al. [5] with the distribution which we calculate using our jet parametrization.

As Ellis et al. [5], we assume that the jets contain 60% charged particles. The data of Ref. [12] corresponds to trigger transverse momenta 2.3 GeV/$c \leqslant q_{\perp t} \leqslant$ 3.3 GeV/c, with $q_{\perp t} = 3.3$ GeV/c dominating near $x_e \lesssim 0.4$ and lower trigger momenta dominating around $x_e \simeq 1$. Therefore we plot the calculated curves for trigger momenta 2, 2.6 and 3.2 GeV/c. Similar to Ellis et al. we find the calculated curves at large x_e bigger than the data but the disagreement is less dramatic than the factor 2 found in Ref. [5].

The paper is organized as follows: In Section 2 we give details about jet production and jet fragmentation. In Section 3 we derive expressions for one-, two-, and three -particle distributions in large transverse momentum and in rapidity, and in Section 4 we discuss the rapidity distributions, compare them with data and work out the rapidity correlation length for two large transverse momentum particles from the same jet. Section 5 summarizes our points.

2. Production and fragmentation of jets

2.1. Jet production

In the hard collision model (Fig. 1) jets are produced by the collision of two constituents i and j belonging to the incoming hadrons A and B. The two-jet production cross section was already discussed by Bjorken [6]

$$E_s E_o \frac{d^6\sigma_J}{d^3P_s d^3P_o} \approx \frac{1}{\pi} \sum_{i,j} f_{iA}(x_1) f_{jB}(x_2) \frac{d\sigma_{ij}(s', t')}{dt'} \delta^{(2)}(P_{\perp s} + P_{\perp o}). \tag{2.1}$$

E_s (E_o) and $P_s(P_o)$ are the energy and momentum of the same side (opposite side) jet. The function $f_{iA}(x_1)$ [$f_{jB}(x_2)$] describes the fragmentation of the incoming hadron $A(B)$ into constituents i (j) where the constituent i (j) carries the fraction $x_1(x_2)$ of the momentum of the incoming hadron A (B). s', t', and u' are the Mandelstam variables for the collision of these constituents i and j. We denote the jet momenta and angles in the overall c.m.s. by $P_{\perp s}$, $P_{\perp o}$, θ_s and θ_o. s', t', x_1 and x_2 can be expressed in terms of these variables [6]

$$s' \approx P_\perp^2 \left(1+\tan\frac{\theta_s}{2}\operatorname{ctg}\frac{\theta_o}{2}\right)\left(1+\tan\frac{\theta_o}{2}\operatorname{ctg}\frac{\theta_s}{2}\right)$$

$$t' \approx -P_\perp^2 \left(1+\tan\frac{\theta_s}{2}\operatorname{ctg}\frac{\theta_o}{2}\right),$$

$$x_1 \approx \frac{P_\perp}{\sqrt{s}}\left(\operatorname{ctg}\frac{\theta_s}{2}+\operatorname{ctg}\frac{\theta_o}{2}\right), \quad x_2 \approx \frac{P_\perp}{\sqrt{s}}\left(\tan\frac{\theta_s}{2}+\tan\frac{\theta_o}{2}\right). \tag{2.2}$$

$d\sigma_{ij}/dt'$ is the differential cross section for the scattering of the constituents i and j. It contains the dynamics of the hard collision process [7–10]

$$\frac{d\sigma_{ij}}{dt'} = \left(\frac{1}{s'}\right)^2 |A(i+j \to s+o)|^2. \tag{2.3}$$

In our calculation we neglect the mass of the jet and approximate

$$\frac{d^3P}{E} \approx PdPd\cos\theta_J d\phi = \frac{P_\perp}{\sin\theta_J} dP_\perp d\theta_J d\phi. \tag{2.4}$$

In this approximation, Eq. (2.1) takes the form

$$\frac{d^4\sigma_J}{dP_{\perp s}dP_{\perp o}d\theta_{Js}d\theta_{Jo}} = \frac{\Delta\phi P_{\perp s}P_{\perp o}}{\sin\theta_{Jo}\sin\theta_{Js}}\left[\frac{1}{\pi}\sum_{i,j} f_{iA}(x_1)f_{jB}(x_2)\frac{d\sigma_{ij}}{dt'}\delta(P_{\perp s}+P_{\perp o})\right). \tag{2.5}$$

In fact, this is only a function of one transverse momentum, such that

$$\frac{d^3\sigma_J}{dP_\perp d\theta_{Js}d\theta_{Jo}} = \frac{\Delta\phi P_\perp^2}{\sin\theta_{Jo}\sin\theta_{Js}}\frac{1}{\pi}\sum_{i,j} f_{iA}(x_1)f_{jB}(x_2)\frac{d\sigma_{ij}}{dt'} \equiv W(P_\perp, \theta_{Js}, \theta_{Jo}, \sqrt{s}). \tag{2.6}$$

The jet production cross section depends on the nature of the constituents and the dynamics of their scattering. The investigation of this dynamics is the central problem of large transverse momentum collisions. Present experimental data is difficult to understand in terms

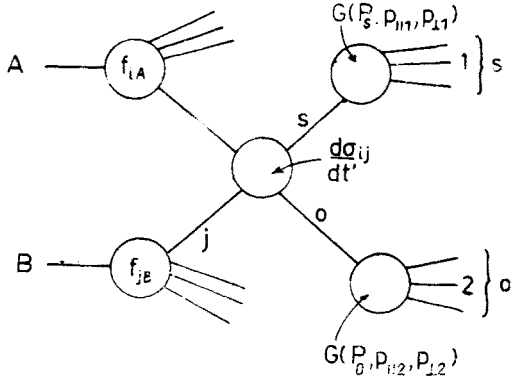

Fig. 2. The hard scattering mechanism explained in the text

of any of the proposed hard scattering mechanisms. In this paper — as in I — we do not try to find the proper dynamics, but rather study only kinematical properties of jets.

In order to illustrate the two-jet cross section we introduce the parametrization of Barger and Phillips [11] for the function $f_{iA}(x_1)$ $\{f_{jB}(x_2)\}$ and for $\frac{d\sigma_{ij}}{dt'}$ we use phase space weighted with $A \sim 1/s'$. For quark-antiquark scattering we obtain at fixed $P_\perp$ the two-jet production cross section plotted in Fig. 3 in form of a contour plot in the θ_{Js}, θ_{Jo} plane. In the large angle region $\theta_{Js} \simeq \theta_{Jo} \simeq \frac{\pi}{2}$ this distribution is almost independent of θ_{Js} and θ_{Jo}.

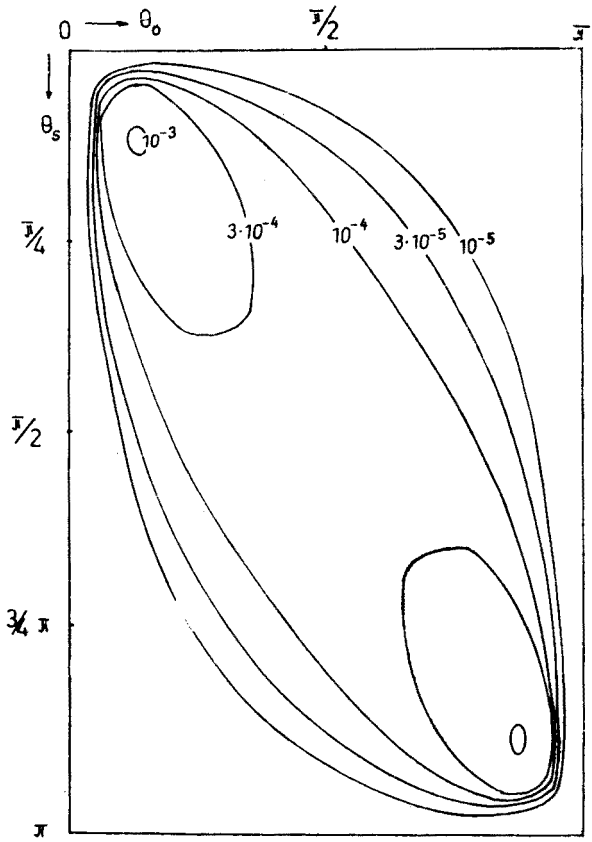

Fig. 3. Contour plot of the two-jet production cross section $W(P_\perp, \theta_{Js}, \theta_{Jo}, \sqrt{s})$ for $P_\perp = 2.65$ GeV/c and $\sqrt{s} = 50$ GeV calculated according to Eq. (2.6) using the parametrization of Ref. [11] for quark (valence + sea) – antiquark (sea only) scattering

For phenomenological purposes we might use as in I an empirical parametrization of the jet production cross section

$$W(P_\perp, \theta_{Js}, \theta_{Jo}, \sqrt{s}) = \frac{\Delta\phi \cdot c}{\sin\theta_{Js} \cdot \sin\theta_{Jo}} \frac{1}{P_\perp^N} \exp\left(-\frac{2DP_\perp}{\sqrt{s}}\right) \tag{2.7}$$

which is independent of θ_{Js} and θ_{Jo} in the central region.

2.2. Jet fragmentation

As in I we describe the jet fragmentation into particles of kind ν by the distribution

$$G_\nu(P, p_\parallel, p_\perp) = \mathscr{E}\frac{d^3n}{d^3p} = n_\nu B\left(1 - \frac{p_\parallel}{P + \frac{A^2}{P}}\right)^F \exp\left(-\frac{p_\parallel^2}{b^2 + \frac{P^4}{M^2}} - \frac{p_\perp^2}{b^2}\right). \tag{2.8}$$

Again, P is the total jet momentum and $\mathscr{E}$ and p are energy and momentum of the considered particle ν in the jet system. B is determined from the energy sum rule assuming the same

kind of distribution for all kinds of particles (see I). The parameters b, F, M, A have been determined by a fit to SPEAR data for charged particles (see I)

$$b = 0.355\ \text{GeV}/c, \qquad M = 0.9\ \text{GeV}, \tag{2.9}$$
$$F = 2, \qquad A = 1.6\ \text{GeV}/c.$$

$n_v = n_{ch}$ is the fraction of charged secondaries. The fit gives $n_{ch} = 0.7$ for $E_{cm} = 3$ GeV and $n_{ch} = 0.5$ for $E_{cm} = 7.4$ GeV, quite in agreement with the increasing neutral excess found by experiments.

To simplify the calculation of same side and opposite side particle distributions as functions of $q_\perp$ and y ($q_\perp$ and y are the c.m.s. transverse momentum and the c.m.s. rapidity of the particle considered) in Sections 3 and 4 we consider all particles to have the same azimuthal angle ϕ as the jet. Therefore we introduce the two transverse momentum components $p_{\perp x}$ and $p_{\perp y}$ in the jet system and integrate over $p_{\perp y}$. Neglecting $p_{\perp y}$ in the energy $\mathscr{E}$, this gives

$$\mathscr{E}\frac{d^2n}{dp_\parallel dp_{\perp x}} = b\sqrt{\pi}\, G(P, p_\parallel, p_{\perp x}). \tag{2.10}$$

For approximate analytical calculation we use the simplified jet fragmentation function (neglecting the deviations from scaling in Eq. (2.5)

$$G'(P, p_\parallel, p_\perp) = \frac{F+1}{\pi b^2}\left(1 - \frac{p_\parallel}{P}\right)^F \exp\left(-\frac{p_\perp^2}{b^2}\right). \tag{2.11}$$

Following I, the two-particle distribution in jet decay is assumed to be uncorrelated

$$\mathscr{E}_1\mathscr{E}_2\frac{d^6n}{d^3p_1 d^3p_2} = \frac{\langle n(n-1)\rangle_J}{\langle n\rangle_J^2} G(P, p_{\parallel 1}, p_{\perp 1})G(P, p_{\parallel 2}, p_{\perp 2}). \tag{2.12}$$

3. The calculation of distributions at large transverse momentum taking into account the transverse momentum distribution within the jet

In this Section we derive expressions for inclusive single particle distributions, same side and opposite side two-particle distributions as well as three-particle distributions in the hard collision model. This model gives the mechanism for jet production and fragmentation and was described in Section 2.

3.1. Same side two-particle cross section

First we discuss the calculation in detail for the distribution of two particles on the same hemisphere (both particles result from the jet s). The same method can be applied for all other distributions mentioned; for these we only give the results.

The invariant distribution of two particles in the same hemisphere is obtained by folding jet production and jet decay. We consider in the jet fragmentation Eq. (2.10) only momentum components within the collision plane (determined by the incoming

hadrons and the two jets). Therefore we obtain the invariant two-particle distribution within this plane

$$q_1^0 q_2^0 \frac{d^4\sigma}{dq_{\parallel 1}dq_{\parallel 2}dq_{\perp 1}dq_{\perp 2}q_{\perp 1}q_{\perp 2}} \equiv \mathscr{J}_{2s}$$

$$= \int_{q_{\perp x_1}+q_{\perp x_2}}^{\sqrt{s/2}} dP_\perp \int_{\theta_s^{(1)}}^{\theta_s^{(2)}} d\theta_{J_s} \int_{\theta_o^{(1)}}^{\theta_o^{(2)}} d\theta_{J_o} \frac{d^3\sigma_J}{dP_\perp d\theta_{J_s} d\theta_{J_o}}$$

$$\times \int dp_{\parallel 1}dp_{\perp x_1}dp_{\parallel 2}dp_{\perp x_2} \frac{d^2n}{dp_{\parallel 1}dp_{\perp x_1}} \frac{d^2n}{dp_{\parallel 2}dp_{\perp x_2}} \frac{\langle n(n-1)\rangle_J}{\langle n\rangle_J^2}$$

$$\times \delta\left(\vartheta_1 - \left[\theta_{J_s} + \operatorname{arctg}\frac{p_{\perp x_1}}{p_{\parallel 1}}\right]\right) \delta(q_{\perp x_1} - [p_{\parallel 1}\sin\theta_{J_s} + p_{\perp x_1}\cos\theta_{J_s}])$$

$$\times \delta\left(\vartheta_2 - \left[\theta_{J_s} + \operatorname{arctg}\frac{p_{\perp x_2}}{p_{\parallel 2}}\right]\right) \delta(q_{\perp x_2} - [p_{\parallel 2}\sin\theta_{J_s} + p_{\perp x_2}\cos\theta_{J_s}]). \tag{3.1}$$

q_i and ϑ_i ($i = 1, 2$) denote the momentum and angle of particle i in the c. m. s. They are related to the momentum and angle in the jet system by (see Fig. 4)

$$\vartheta = \theta_{J_s} + \bar{\vartheta} = \theta_{J_s} + \operatorname{arctg}\frac{p_{\perp x}}{p_\parallel} \tag{3.2}$$

and

$$q_\perp = p_\parallel \sin\theta_{J_s} + p_{\perp x}\cos\theta_{J_s}, \tag{3.3}$$

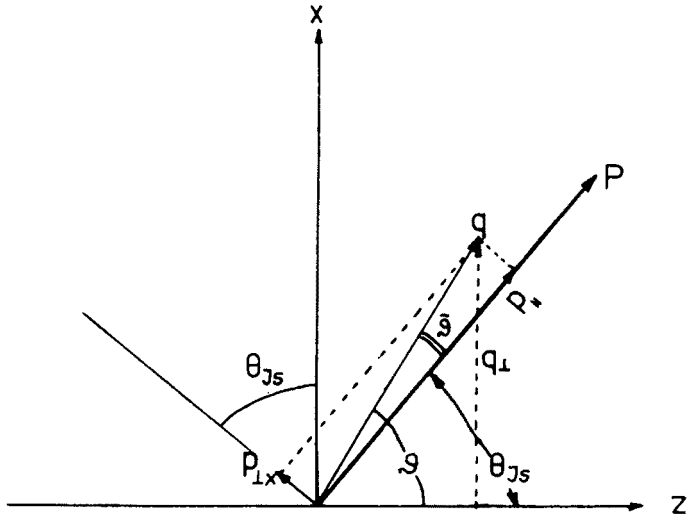

Fig. 4. The relation between the variables in the jet system $p_{\parallel}, p_{\perp x}, \bar{\vartheta}$ and the c. m. s. variables $q, q_\perp, \vartheta$ and the jet variables P and θ_{J_s}

where all particles are in the x, z plane with $\phi = 0$. These relations are expressed by the δ functions in Eq. (3.1). The limits of integration for the polar angles θ_{Js} and θ_{Jo} of the jets are obtained from energy momentum conservation.

The transverse momenta of the two jets are always identical within the hard collision model. The conservation of longitudinal momentum can be written in the form

$$P_{\|o}+P_{\|s} = P_{\|c}, \tag{3.4}$$

where $P_{\|o}$ ($P_{\|s}$) is the longitudinal momentum of the opposite (same) side jet

$$P_{\|s(o)} = P_{\perp} \operatorname{ctg} \theta_{Js(o)}. \tag{3.5}$$

$P_{\|c}$ is the longitudinal momentum of the low transverse momentum component which is present in general. We write energy conservation in the form

$$\sqrt{P_{\|o}^2+P_{\perp}^2} + \sqrt{P_{\|s}^2+P_{\perp}^2} + \sqrt{P_{\|c}^2} = \sqrt{s}. \tag{3.6}$$

Here we assume the mass of the jets and the invariant mass of the low transverse momentum component are negligible at the kinematic limit. We determine the kinematical limit for θ_{Js} from the requirement

$$P_s = \frac{P_{\perp}}{\sin \theta_{Js}} \leqslant \frac{\sqrt{s}}{2} \tag{3.7}$$

and obtain

$$\theta_s^{(1)} = \arcsin \frac{2P_{\perp}}{\sqrt{s}},$$

$$\theta_s^{(2)} = \pi - \arcsin \frac{2P_{\perp}}{\sqrt{s}}. \tag{3.8}$$

For given $P_{\|s}$ we determine the kinematical limits for $P_{\|o}$ from Eqs (3.4) and (3.6); they are

$$P_{\|o} = \frac{1}{a}(-b \pm \sqrt{b^2+ac})$$

with

$$\begin{aligned} a &= 4(s+P_{\perp}^2-2\sqrt{s}\sqrt{P_{\|s}^2+P_{\perp}^2}), \\ b &= 2P_{\|s}(s+2P_{\perp}^2-2\sqrt{s}\sqrt{P_{\|s}^2+P_{\perp}^2}), \\ c &= s^2+4sP_{\|s}^2+4sP_{\perp}^2-4P_{\perp}^2P_{\|s}^2-4s\sqrt{s}\sqrt{P_{\|s}^2+P_{\perp}^2}. \end{aligned} \tag{3.9}$$

$P_{\|s}$ is given by Eq. (3.5). We obtain $\theta_o^{(1)}$ and $\theta_o^{(2)}$ according to

$$\theta_o^{(1)} = \operatorname{arctg}\left(\frac{P_{\|o1}}{P_{\perp}}\right),$$

$$\theta_o^{(2)} = \operatorname{arctg}\left(\frac{P_{\|o2}}{P_{\perp}}\right). \tag{3.10}$$

We insert the expression for $\frac{d^3\sigma_J}{dP_\perp d\theta_{Js} d\theta_{Jo}}$ given in Eq. (2.6) and the expression for $\frac{d^2n}{dp_{\|i} dp_{\perp xi}}$ $(i = 1, 2)$ obtained from Eq. (2.10) putting approximately $\mathscr{E}_i \approx p_i$.

We have

$$\mathscr{J}_{2s} = \pi b^2 \int_{q_{\perp x_1}+q_{\perp x_2}}^{\sqrt{s/2}} dP_\perp \int_{\theta_s^{(1)}}^{\theta_s^{(2)}} d\theta_{Js} \int_{\theta_o^{(1)}}^{\theta_o^{(2)}} d\theta_{Jo} W(P_\perp, \theta_{Js}, \theta_{Jo}, \sqrt{s})$$

$$\times \int dp_{\|1} dp_{\|2} dp_{\perp x_1} dp_{\perp x_2} \frac{1}{p_{\|1}} \frac{1}{p_{\|2}} G\left(\frac{P_\perp}{\sin\theta_{Js}}, p_{\|1}, p_{\perp x_1}\right) G\left(\frac{P_\perp}{\sin\theta_{Js}}, p_{\|2}, p_{\perp x_2}\right)$$

$$\times \frac{\langle n(n-1)\rangle_J}{\langle n\rangle_J^2} \delta\left(\vartheta_1 - \left[\theta_{Js} + \operatorname{arctg}\frac{p_{\perp x_1}}{p_{\|1}}\right]\right) \delta\left(\vartheta_2 - \left[\theta_{Js} + \operatorname{arctg}\frac{p_{\perp x_2}}{p_{\|2}}\right]\right)$$

$$\times \delta(q_{\perp x_1} - [p_{\|1} \sin\theta_{Js} + p_{\perp x_1} \cos\theta_{Js}]) \delta(q_{\perp x_2} - [p_{\|2} \sin\theta_{Js} + p_{\perp x_2} \cos\theta_{Js}]). \quad (3.11)$$

We integrate first over $p_{\perp x_1}$ and $p_{\perp x_2}$ using the δ functions with the ϑ_i variables $(i = 1, 2)$, with

$$\mathscr{J}_{2s} = \pi b^2 \int_{q_{\perp x_1}+q_{\perp x_2}}^{\sqrt{s/2}} dP_\perp \int_{\bar\theta_s^{(1)}}^{\bar\theta_s^{(2)}} d\theta_{Js} \int_{\theta_o^{(1)}}^{\theta_o^{(2)}} d\theta_{Jo} W(P_\perp, \theta_{Js}, \theta_{Jo}, \sqrt{s}) \frac{\langle n(n-1)\rangle_J}{\langle n\rangle_J^2}$$

$$\times \frac{1}{\cos^2(\vartheta_1 - \theta_{Js}) \cos^2(\vartheta_2 - \theta_{Js})} G\left(\frac{P_\perp}{\sin\theta_{Js}}, p_{\|1}, p_{\|1} \operatorname{tg}(\vartheta_1 - \theta_{Js})\right)$$

$$\times G\left(\frac{P_\perp}{\sin\theta_{Js}}, p_{\|2}, p_{\|2} \operatorname{tg}(\vartheta_2 - \theta_{Js})\right) \delta\left(q_{\perp 1} - p_{\|1} \frac{\sin\vartheta_1}{\cos(\vartheta_1 - \theta_{Js})}\right)$$

$$\times \delta\left(q_{\perp 2} - p_{\|2} \frac{\sin\vartheta_2}{\cos(\vartheta_2 - \theta_{Js})}\right). \quad (3.12)$$

with

$$\bar\theta_s^{(1)} = \max\left(\theta_s^{(1)}, \vartheta_1 - \frac{\pi}{2}, \vartheta_2 - \frac{\pi}{2}\right),$$

$$\bar\theta_s^{(2)} = \min\left(\theta_s^{(2)}, \vartheta_1 + \frac{\pi}{2}, \vartheta_2 + \frac{\pi}{2}\right), \quad (3.13)$$

We integrate over $dp_{\|_1}$ and $dp_{\|_2}$ using the δ-functions and obtain

$$-q_1^0 q_2^0 \left.\frac{d^4\sigma}{dq_{\|1} dq_{\|2} q_{\perp 1} q_{\perp 2} dq_{\perp 1} dq_{\perp 2}}\right|_{\text{same}} \equiv \mathscr{J}_{2s}$$

$$= \pi b^2 \int_{q_{\perp 1}+q_{\perp 2}}^{\sqrt{s/2}} dP_\perp \int_{\bar\theta_s^{(1)}}^{\bar\theta_s^{(2)}} d\theta_{Js} \int_{\theta_o^{(1)}}^{\theta_o^{(2)}} d\theta_{Jo} \frac{1}{\cos(\vartheta_1 - \theta_{Js}) \cos(\vartheta_2 - \theta_{Js}) \sin\vartheta_1 \sin\vartheta_2}$$

$$\times \frac{\langle n(n-1)\rangle_J}{\langle n\rangle_J^2} W(P_\perp, \theta_{J_s}, \theta_{J_o}, \sqrt{s}) G\left(\frac{P_\perp}{\sin\theta_{J_s}}, q_{\perp 1}\frac{\cos(\vartheta_1-\theta_{J_s})}{\sin\vartheta_1}, q_{\perp 1}\frac{\sin(\vartheta_1-\theta_{J_s})}{\sin\vartheta_1}\right)$$

$$\times G\left(\frac{P_\perp}{\sin\theta_{J_s}}, q_{\perp 2}\frac{\cos(\vartheta_2-\theta_{J_s})}{\sin\vartheta_2}, q_{\perp 2}\frac{\sin(\vartheta_2-\theta_{J_s})}{\sin\vartheta_2}\right). \tag{3.14}$$

This expression can be evaluated numerically or by use of suitable approximations for the functions W and G. We shall return to Eq. (3.14) in the next Section. Using the same methods as for the same side correlations we calculate the following other distributions:

3.2. Single particle cross section

$$q^0\frac{d^2\sigma}{dq_\parallel q_\perp dq_\perp} = \int_{q_\perp}^{\sqrt{s/2}} dP_\perp \int_{\theta_s^{(1)}}^{\theta_s^{(2)}} d\theta_{J_s} \int_{\theta_o^{(1)}}^{\theta_o^{(2)}} d\theta_{J_o} W(P_\perp, \theta_{J_s}, \theta_{J_o}, \sqrt{s})$$

$$\times b\sqrt{\pi}\int dp_\parallel dp_{\perp x}\frac{1}{\mathscr{E}} G\left(\frac{P_\perp}{\sin\theta_{J_s}}, p_\parallel, p_{\perp x}\right)\delta\left(\vartheta-\left[\theta_{J_s}+\operatorname{arctg}\frac{p_{\perp x}}{p_\parallel}\right]\right)$$

$$\times\delta(q_\perp-[p_\parallel\sin\theta_{J_s}+p_{\perp x}\cos\theta_{J_s}]). \tag{3.15}$$

Integrating we obtain

$$q^0\frac{d^2\sigma}{dq_\parallel q_\perp dq_\perp} = b\sqrt{\pi}\int_{q_\perp}^{\sqrt{s/2}} dP_\perp \int_{\bar\theta_s^{(1)}}^{\bar\theta_s^{(2)}} d\theta_{J_s} \int_{\theta_o^{(1)}}^{\theta_o^{(2)}} d\theta_{J_o}\frac{1}{\cos(\vartheta_1-\theta_{J_s})}$$

$$\times\frac{1}{\sin\vartheta} W(P_\perp, \theta_{J_s}, \theta_{J_o}, \sqrt{s}) G\left(\frac{P_\perp}{\sin\theta_{J_s}}, q_\perp\frac{\cos(\vartheta-\theta_{J_s})}{\sin\vartheta}, q_\perp\frac{\sin(\vartheta-\theta_{J_s})}{\sin\vartheta}\right), \tag{3.16}$$

where $\bar\theta_s^{(1)}$, $\bar\theta_s^{(2)}$ and $\theta_o^{(1)}$, $\theta_o^{(2)}$ are defined as in Eqs (3.8), (3.10) and (3.13), but all terms with ϑ_2 are dropped.

3.3. Opposite side two-particle cross section

(particle 1 is the trigger (side s), particle 2 is on the opposite side o)

$$q_1^0 q_2^0\frac{d^4\sigma}{dq_{\parallel 1}dq_{\parallel 2}q_{\perp 1}q_{\perp 2}dq_{\perp 1}dq_{\perp 2}}\bigg|_{\text{opposite}} = \pi b^2\int_{\theta_\perp}^{\sqrt{s/2}} dP_\perp \int_{\theta_s^{(1)}}^{\theta_s^{(2)}} d\theta_{J_s}$$

$$\times\int_{\theta_o^{(1)}}^{\theta_o^{(2)}} d\theta_{J_o} W(P_\perp, \theta_{J_s}, \theta_{J_o}, \sqrt{s})\int dp_{\parallel 1}dp_{\parallel 2}dp_{\perp x_1}dp_{\perp x_2}\frac{1}{\mathscr{E}_1\mathscr{E}_2} G\left(\frac{P_\perp}{\sin\theta_{J_s}}, p_{\parallel 1}, p_{\perp x_1}\right)$$

$$\times G\left(\frac{P_\perp}{\sin\theta_{J_o}}, p_{\parallel 2}, p_{\perp x_2}\right)\delta\left(\vartheta_1-\left[\theta_{J_s}+\operatorname{arctg}\frac{p_{\perp x_1}}{p_{\parallel 1}}\right]\right)$$

$$\times\delta\left(\vartheta_2-\left[\theta_{J_o}+\operatorname{arctg}\frac{p_{\perp x_2}}{p_{\parallel 2}}\right]\right)\delta(q_{\perp 1}-[p_{\parallel 1}\sin\theta_{J_s}+p_{\perp x_1}\cos\theta_{J_s}])$$

$$\times\delta(q_{\perp 2}-[p_{\parallel 2}\sin\theta_{J_o}+p_{\perp x_2}\cos\theta_{J_o}]). \tag{3.17}$$

It is

$$Q_\perp = \begin{cases} q_{\perp 1} & \text{for} \quad q_{\perp 1} \geqslant q_{\perp 2}, \\ q_{\perp 2} & \text{for} \quad q_{\perp 2} \geqslant q_{\perp 1}. \end{cases} \tag{3.18}$$

Integrating as above we obtain

$$q_1^0 q_2^0 \frac{d^4\sigma}{dq_{\parallel 1} dq_{\parallel 2} q_{\perp 1} q_{\perp 2} dq_{\perp 1} dq_{\perp 2}}\Bigg|_{\text{opposite}}$$

$$= \pi b^2 \int_{Q_\perp}^{\sqrt{s/2}} dP_\perp \int_{\bar\theta_s^{(1)}}^{\bar\theta_s^{(2)}} d\theta_{J_s} \int_{\bar\theta_o^{(1)}}^{\bar\theta_o^{(2)}} d\theta_{J_o} \frac{1}{\cos(\vartheta_1 - \theta_{J_s}) \cos(\vartheta_2 - \theta_{J_o}) \sin\vartheta_1 \sin\vartheta_2}$$

$$\times W(P_\perp, \theta_{J_s}, \theta_{J_o}, \sqrt{s}) G\left(\frac{P_\perp}{\sin\theta_{J_s}}, q_{\perp 1} \frac{\cos(\vartheta_1 - \theta_{J_s})}{\sin\vartheta_1}, q_{\perp 1} \frac{\sin(\vartheta_1 - \theta_{J_s})}{\sin\vartheta_1}\right)$$

$$\times G\left(\frac{P_\perp}{\sin\theta_{J_o}}, q_{\perp 2} \frac{\cos(\vartheta_2 - \theta_{J_o})}{\sin\vartheta_2}, q_{\perp 2} \frac{\sin(\vartheta_2 - \theta_{J_o})}{\sin\vartheta_2}\right). \tag{3.19}$$

The limits of integration $\theta_s^{(i)}$ and $\theta_o^{(i)}$ $(i = 1, 2)$ are given in Eqs (3.8) and (3.10). Furthermore

$$\bar\theta_s^{(1)} = \max\left(\theta_s^{(1)}, \vartheta_1 - \frac{\pi}{2}\right), \quad \bar\theta_s^{(2)} = \min\left(\pi - \theta_s^{(1)}, \vartheta_1 + \frac{\pi}{2}\right),$$

$$\bar\theta_o^{(1)} = \max\left(\theta_o^{(1)}, \vartheta_2 - \frac{\pi}{2}\right), \quad \bar\theta_o^{(2)} = \min\left(\bar\theta_o^{(2)}, \vartheta_2 + \frac{\pi}{2}\right). \tag{3.20}$$

3.4. Opposite side three-particle cross section

(particle 1 is the trigger, side s; particle 2 and 3 are on the opposite side o)

$$q_1^0 q_2^0 q_3^0 \frac{d^6\sigma}{dq_{\parallel 1} dq_{\parallel 2} dq_{\parallel 3} q_{\perp 1} q_{\perp 2} q_{\perp 3} dq_{\perp 1} dq_{\perp 2} dq_{\perp 3}}\Bigg|_{\text{opposite}}$$

$$= \int_{Q_\perp}^{\sqrt{s/2}} dP_\perp \int_{\theta_s^{(1)}}^{\theta_s^{(2)}} d\theta_{J_s} \int_{\theta_o^{(1)}}^{\theta_o^{(2)}} d\theta_{J_o} W(P_\perp, \theta_{J_s}, \theta_{J_o}, \sqrt{s}) \int dp_{\parallel 1} dp_{\parallel 2} dp_{\parallel 3}$$

$$\times \int dp_{\perp x_1} dp_{\perp x_2} dp_{\perp x_3} \frac{b^3\pi^{3/2}}{\mathscr{E}_1 \mathscr{E}_2 \mathscr{E}_3} G\left(\frac{P_\perp}{\sin\theta_{J_s}}, p_{\parallel 1}, p_{\perp x_1}\right) \frac{\langle n(n-1)\rangle_J}{\langle n\rangle_J^2}$$

$$\times G\left(\frac{P_\perp}{\sin\theta_{J_o}}, p_{\parallel 2}, p_{\perp x_2}\right) G\left(\frac{P_\perp}{\sin\theta_{J_o}}, p_{\parallel 3}, p_{\perp x_3}\right)$$

$$\times \delta\left(\vartheta_1 - \left[\theta_{J_s} + \operatorname{arctg}\frac{p_{\perp x_1}}{p_{\parallel 1}}\right]\right) \delta\left(\vartheta_2 - \left[\theta_{J_o} + \operatorname{arctg}\frac{p_{\perp x_2}}{p_{\parallel 2}}\right]\right)$$

$$\times \delta\left(\vartheta_3 - \left[\theta_{J_o} + \operatorname{arctg}\frac{p_{\perp x_3}}{p_{\parallel 3}}\right]\right) \delta(q_{\perp 1} - [p_{\parallel 1} \sin\theta_{J_s} + p_{\perp x_1} \cos\theta_{J_s}])$$

$$\times \delta(q_{\perp 2} - [p_{\parallel 2} \sin\theta_{J_o} + p_{\perp x_2} \cos\theta_{J_s}]) \delta(q_{\perp 3} - [P_{\parallel 3} \sin\theta_{J_o} + p_{\perp x_3} \cos\theta_{J_o}]). \tag{3.21}$$

Further it is

$$Q_\perp = \begin{cases} q_{\perp 1} & \text{for} \quad q_{\perp 1} \geqslant q_{\perp 2}+q_{\perp 3}, \\ q_{\perp 2}+q_{\perp 3} & \text{for} \quad q_{\perp 2}+q_{\perp 3} \geqslant q_{\perp 1}. \end{cases} \tag{3.22}$$

Integrating as above we obtain

$$q_1^0 q_2^0 q_3^0 \frac{d^6\sigma}{dq_{\parallel 1}dq_{\parallel 2}dq_{\parallel 3}q_{\perp 1}q_{\perp 2}q_{\perp 3}dq_{\perp 1}dq_{\perp 2}dq_{\perp 3}}\Big|_{\text{opposite}}$$

$$= \pi^{3/2}b^3 \int_{Q_\perp}^{\sqrt{s/2}} dP_\perp \int_{\bar\theta_s^{(1)}}^{\bar\theta_s^{(2)}} d\theta_{J_s} \int_{\bar\theta_o^{(1)}}^{\bar\theta_o^{(2)}} d\theta_{J_o} \frac{1}{\cos(\vartheta_1-\theta_{J_s})\cos(\vartheta_2-\theta_{J_s})}$$

$$\times \frac{1}{\cos(\vartheta_3-\theta_{J_o})\sin\vartheta_1\sin\vartheta_2\sin\vartheta_3} \frac{\langle (n-1)\rangle_J}{\langle n\rangle_J^2} W(P_\perp, \theta_{J_s}, \theta_{J_o}, \sqrt{s})$$

$$\times G\left(\frac{P_\perp}{\sin\theta_{J_s}}, q_{\perp 1}\frac{\cos(\vartheta_1-\theta_{J_s})}{\sin\vartheta_1}, q_{\perp 1}\frac{\sin(\vartheta_1-\theta_{J_s})}{\sin\vartheta_1}\right)$$

$$\times G\left(\frac{P_\perp}{\sin\theta_{J_o}}, q_{\perp 2}\frac{\cos(\vartheta_2-\theta_{J_o})}{\sin\vartheta_2}, q_{\perp 2}\frac{\sin(\vartheta_2-\theta_{J_o})}{\sin\vartheta_2}\right)$$

$$\times G\left(\frac{P_\perp}{\sin\theta_{J_o}}, q_{\perp 3}\frac{\cos(\vartheta_3-\theta_{J_o})}{\sin\vartheta_3}, q_{\perp 3}\frac{\sin(\vartheta_3-\theta_{J_o})}{\sin\vartheta_3}\right). \tag{3.23}$$

The limits of integration $\theta_s^{(i)}$ and $\theta_o^{(i)}$ $(i = 1, 2)$ are given in Eqs (3.8) and (3.10). Furthermore

$$\bar\theta_s^{(1)} = \max\left(\theta_s^{(1)}, \vartheta_1-\frac{\pi}{2}\right), \quad \bar\theta_s^{(2)} = \min\left(\pi-\theta_s^{(1)}, \vartheta_1+\frac{\pi}{2}\right),$$

$$\bar\theta_o^{(1)} = \max\left(\theta_o^{(1)}, \vartheta_2-\frac{\pi}{2}, \vartheta_3-\frac{\pi}{2}\right),$$

$$\bar\theta_o^{(2)} = \min\left(\theta_s^{(2)}, \vartheta_2+\frac{\pi}{2}, \vartheta_3+\frac{\pi}{2}\right). \tag{3.24}$$

4. Rapidity distributions of large transverse momentum particles

4.1. Same side and opposite side two-particle cross sections

For fixed transverse momentum and rapidity of the trigger particle 1 we obtain the rapidity distribution of a second particle at the same or the opposite hemisphere of the trigger particle by numerical integration of Eqs (3.14) and (3.19). In these calculations we use the jet fragmentation function given in Eq. (2.8). For the jet production cross

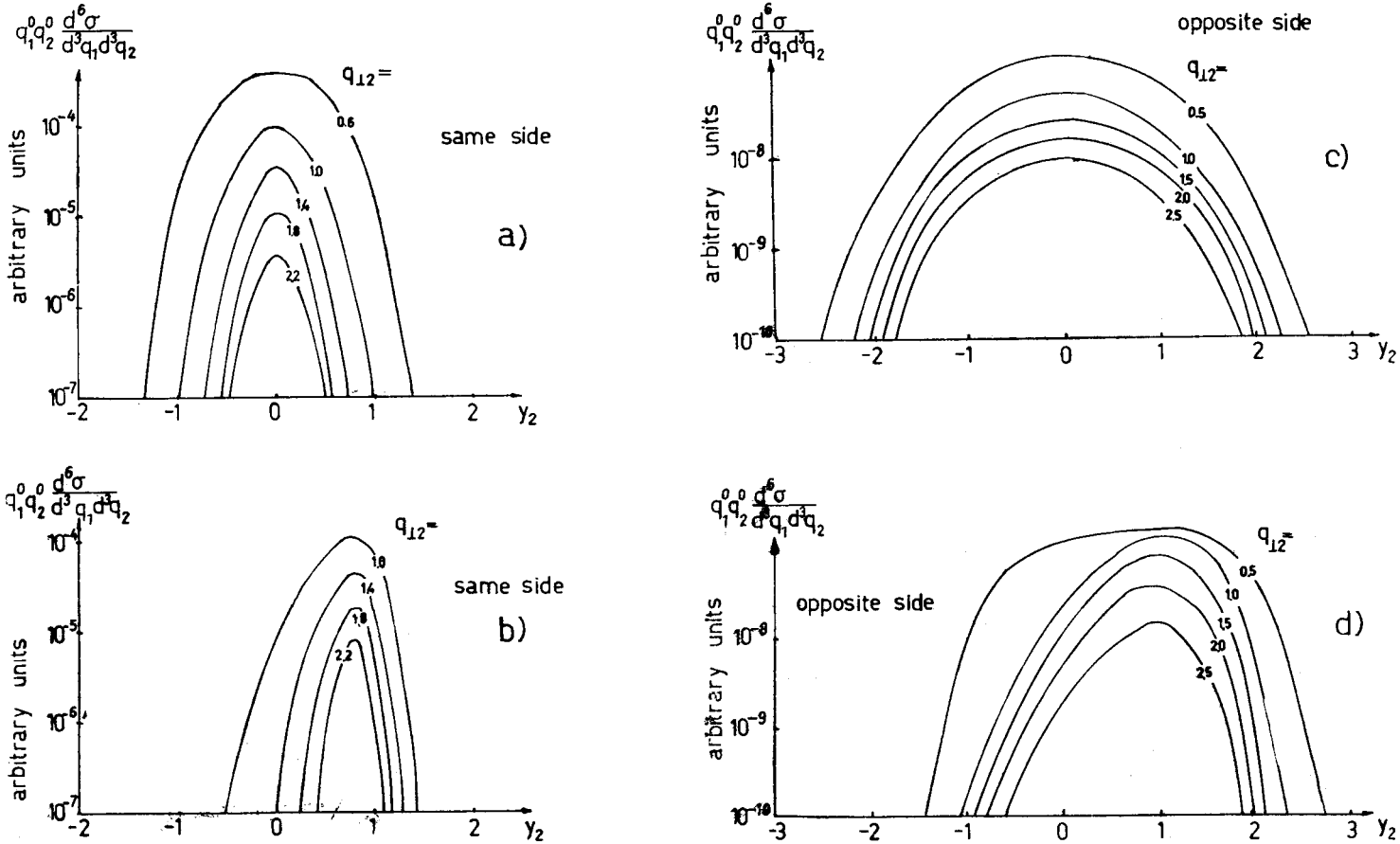

Fig. 5. Comparison of the same side and opposite side two-particle distribution plotted as function of the rapidity of the second particle for fixed transverse momenta of both particles and fixed rapidity of particle 1. a) and b) same side two-particle distribution a) $y_1 = 0, q_{\perp 1} = 2$ GeV/c, b) $y_1 = 1, q_{\perp 1} = 2$ GeV/c; c) and d) opposite side two-particle distribution, c) $y_1 = 0$, $q_{\perp 1} = 4$ GeV/c, d) $y_1 = 0.5$, $q_{\perp 1} = 4$ GeV/c

section we use Eq. (2.6) with the same quark parton densities used for the example plotted in Fig. 3. It is our aim to study the rapidity correlations between same side particles as compared to opposite side particles. This rapidity correlation is mainly a result of the jet fragmentation, in particular the transverse momentum distribution within the jet. Therefore, for this purpose, we do not attach any special importance to the particular form of the jet production cross section. In order to study the dynamics of jet production we would need experimental data on the rapidity y and transverse momentum $q_\perp$ dependence of the single particle distribution and the y and $q_\perp$ dependence of the opposite side distributions as well as quantum number correlations. In Fig. 5 we compare the rapidity distribu-

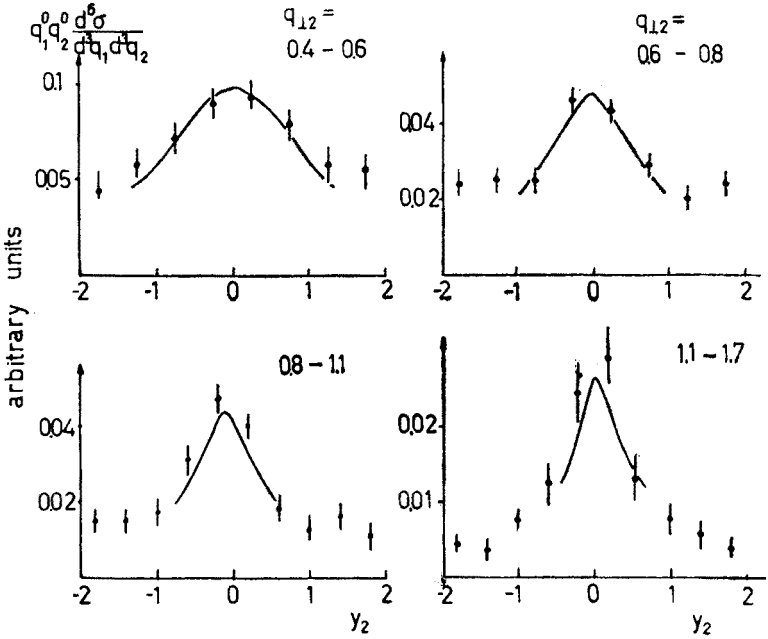

Fig. 6. Same side two-particle distribution plotted as function of the rapidity of the second particle. The trigger particle has the rapidity $y_1 = 0$ and transverse momentum $q_{\perp 1} = 2$ GeV/c. The transverse momentum of the second particle is in the bins indicated on the plots. The calculated curve is compared with data from Ref. [12]

tion of the second particle at the same side or opposite side of the trigger particle. We find this rapidity distribution at the same side rather narrow and centered around the rapidity of the trigger particle. The width of the same side rapidity distribution decreases with the transverse momentum of the second particle. Later on we shall find that the shape of the same side distribution is mainly determined by the details of the jet fragmentation.

The opposite side rapidity distribution is rather wide and reflects mainly the details of the jet production cross section. There is no experimental data available for the opposite side distribution which could be used to study jet production dynamics. Data on the same

side rapidity distribution was measured at the CERN-ISR [12]. In Fig. 6 we compare the measured rapidity distributions for the second particle in different rapidity bins with the calculated distributions and find rather good agreement in particular for the width of the curves and their changes with changing transverse momentum of the second particle. It has, however, to be taken into account that the width of the experimental curve is increased due to the finite angular acceptance of the lead glass detector for the trigger π^0.

4.2. The correlation length in rapidity for two particles from the same side jet

In order to understand the shape of the same side rapidity distribution and its change with transverse momentum qualitatively, we calculate the same side two-particle distribution (3.14) analytically using approximations for jet production and fragmentation.

We use the jet production cross section (2.7) and the simplified jet fragmentation into two particles

$$G'(P, p_{\parallel 1}, p_{\perp 1})G'(P, p_{\parallel 2}, p_{\perp 2}) \approx \frac{(F+1)^2}{\pi^2 b^4}\left(1-\frac{p_{\parallel 1}+p_{\parallel 2}}{P}\right)^F \exp\left(-\frac{p_{\perp 1}^2+p_{\perp 2}^2}{b^2}\right) \tag{4.1}$$

in Eq. (3.14) and obtain

$$\mathcal{J}_{2s} = \frac{d^4\sigma}{q_{\perp 1}q_{\perp 2}dy_1dy_2dq_{\perp 1}dq_{\perp 2}}$$

$$= \int_{q_{\perp 1}+q_{\perp 2}}^{\sqrt{s/2}} dP_\perp \int_{\bar{\theta}_s^{(1)}}^{\bar{\theta}_s^{(2)}} d\theta_{Js} \int_{\theta_o^{(1)}}^{\theta_o^{(2)}} d\theta_{Jo} \frac{1}{\cos(\vartheta_1-\theta_{Js})\cos(\vartheta_2-\theta_{Js})\sin\vartheta_1\sin\vartheta_2}$$

$$\times \frac{1}{\sin\theta_{Js}\sin\theta_{Jo}} \frac{1}{P_\perp^N} \exp\left(-\frac{2DP_\perp}{\sqrt{s}}\right)$$

$$\times \left\{1-\frac{\sin\theta_{Js}}{P_\perp}\left(q_{\perp 1}\frac{\cos(\vartheta_1-\theta_{Js})}{\sin\vartheta_1}+q_{\perp 2}\frac{\cos(\vartheta_2-\theta_{Js})}{\sin\vartheta_2}\right)\right\}^F$$

$$\times \exp\left(-\frac{1}{b^2}\left\{\left(q_{\perp 1}\frac{\sin(\vartheta_1-\theta_{Js})}{\sin\vartheta_1}\right)^2+\left(q_{\perp 2}\frac{\sin(\vartheta_2-\theta_{Js})}{\sin\vartheta_2}\right)^2\right\}\right). \tag{4.2}$$

We are interested in the behaviour for $\vartheta_1 \simeq \vartheta_2 \simeq 90°$. Because of the exponential damping in the last term we can use integration limits $\theta_{Js}^{(1)}, \theta_{Js}^{(2)}, \theta_{Jo}^{(1)}, \theta_{Jo}^{(2)}$ independent of $P_\perp$ and exchange the $P_\perp$ integration with the θ_{Js} and θ_{Jo} integration. Furthermore we transform the $P_\perp$ integral to the variable

$$x = \frac{\sin\theta_{Js}}{P_\perp}\left(q_{\perp 1}\frac{\cos(\vartheta_1-\theta_{Js})}{\sin\vartheta_1}+q_{\perp 2}\frac{\cos(\vartheta_2-\theta_{Js})}{\sin\vartheta_2}\right) \tag{4.3}$$

and obtain in good approximation after integration over θ_{J_0}

$$\mathcal{J}_{2s} = \frac{d^4\sigma}{q_{\perp 1} q_{\perp 2} dq_{\perp 1} dq_{\perp 2} dy_1 dy_2}$$

$$\approx \int_{\bar{\theta}_s^{(1)}}^{\bar{\theta}_s^{(2)}} d\theta_{J_s} \frac{1}{\sin^N \theta_{J_s}} \frac{1}{A^{N-1}} \frac{1}{\sin \vartheta_1 \sin \vartheta_2 \cos(\vartheta_1 - \theta_{J_s}) \cos(\vartheta_2 - \theta_{J_s})}$$

$$\times \exp\left(- \frac{q_{\perp 1}^2}{b^2} \frac{\sin^2(\vartheta_1 - \theta_{J_s})}{\sin^2 \vartheta_1} - \frac{q_{\perp 2}^2}{b^2} \frac{\sin^2(\vartheta_2 - \theta_{J_s})}{\sin^2 \vartheta_2} \right) \times \mathcal{K} \tag{4.4}$$

with

$$A = q_{\perp 1} \frac{\cos(\vartheta_1 - \theta_{J_s})}{\sin \vartheta_1} + q_{\perp 2} \frac{\cos(\vartheta_2 - \theta_{J_s})}{\sin \vartheta_2} . \tag{4.5}$$

The function $\mathcal{K}$ is the x integral

$$\mathcal{K} = \int_0^1 dx\, x^{N-2} \exp\left(- \frac{2D \sin \theta_{J_s}}{x \sqrt{s}} A \right) (1-x)^F \tag{4.6}$$

which can be approximated (see I) by

$$\mathcal{K} \approx \frac{F!(N-2)!}{(F+N-1)!} \exp\left(- \frac{2D \sin \theta_{J_s}}{\sqrt{s}} A \right). \tag{4.7}$$

We want to find the shape of the rapidity distribution of particle 2 for the trigger particle 1 at fixed transverse momentum and fixed angle $\vartheta_1 = 90°$ and for a given fixed transverse momentum $q_{\perp 2}$ of the second particle. In this case we have

$$\sin \vartheta_1 = 1,$$

$$\sin(\vartheta_1 - \theta_{J_s}) = \cos \theta_{J_s},$$

$$\cos(\vartheta_1 - \theta_{J_s}) = \sin \theta_{J_s},$$

$$\frac{\cos(\vartheta_2 - \theta_{J_s})}{\sin \vartheta_2} = \operatorname{ctg} \vartheta_2 \cos \theta_{J_s} + \sin \theta_{J_s},$$

$$\frac{\sin(\vartheta_2 - \theta_{J_s})}{\sin \vartheta_2} = \cos \theta_{J_s} - \operatorname{ctg} \vartheta_2 \sin \theta_{J_s}. \tag{4.8}$$

Furthermore we approximate

$$\cos(\vartheta_2 - \theta_{J_s}) \approx \sin \vartheta_2 \sin \theta_{J_s} \tag{4.9}$$

and neglect the exponential function $\exp\left(-\frac{2D\sin\theta_{J_s}}{\sqrt{s}}A\right)$ resulting from the jet production term which does not dominate the ϑ_2 dependence. We have

$$\mathcal{J}_{2s} \sim \int_{\bar{\theta}_s^{(1)}}^{\bar{\theta}_s^{(2)}} d\theta_{J_s} \frac{1}{(\sin\theta_{J_s})^{N+2}} \frac{1}{\sin^2\vartheta_2}$$
$$\times [q_{\perp 1}\sin\theta_{J_s} + q_{\perp 2}\sin\theta_{J_s} + q_{\perp 2}\cos\theta_{J_s}\operatorname{ctg}\vartheta_2]^{1-N}$$
$$\times \exp\left[-\frac{1}{b^2}(q_{\perp 1}^2\cos^2\theta_{J_s} + q_{\perp 2}^2\{\cos\theta_{J_s} - \sin\theta_{J_s}\operatorname{ctg}\vartheta_2\}^2)\right]. \tag{4.10}$$

We transform the integration to $d\cos\theta_{J_s} = dz$ and keep only the exponential function. This gives

$$\mathcal{J}_{2s} \sim \int dz \exp\left[-\frac{z^2}{b^2}(q_{\perp 1}^2 + q_{\perp 2}^2 - q_{\perp 2}^2\operatorname{ctg}^2\vartheta_2)\right.$$
$$\left. + 2\frac{z}{b^2}q_{\perp 2}^2\operatorname{ctg}\vartheta_2 - \frac{q_{\perp 2}^2}{b^2}\operatorname{ctg}^2\vartheta_2\right]. \tag{4.11}$$

We have kept only terms up to z^2 in the exponent. Due to the large values of $q_{\perp i}$ $(i = 1, 2)$ and the small size of b we can extend the integration limits to infinity and obtain

$$\mathcal{J}_{2s} \sim \exp\left[-\frac{\operatorname{ctg}^2\vartheta_2}{b^2}\frac{q_{\perp 1}^2 - q_{\perp 2}^2\operatorname{ctg}^2\vartheta_2}{1 + \frac{q_{\perp 1}^2}{q_{\perp 2}^2} - \operatorname{ctg}^2\vartheta_2}\right]. \tag{4.12}$$

We transform Eq. (4.12) to c. m. s. rapidity variables. For small y_2 we have $y_2 \approx \operatorname{ctg}\vartheta_2$. We also neglect the two terms in curled brackets containing $\operatorname{ctg}^2\vartheta$. We then have finally

$$\mathcal{J}_{2s} = \frac{d^4\sigma}{q_{\perp 1}q_{\perp 2}dq_{\perp 1}dq_{\perp 2}dy_1dy_2}\bigg|_{y_1\approx 0} \simeq \exp\left[-\frac{y^2}{b^2}\cdot\frac{q_{\perp 1}^2 q_{\perp 2}^2}{q_{\perp 1}^2 + q_{\perp 2}^2}\right]. \tag{4.13}$$

We thus find short range correlation between y_1 and y_2 with a correlation length

$$L(q_{\perp 1}, q_{\perp 2}) = \frac{b}{\sqrt{2}}\frac{\sqrt{q_{\perp 1}^2 + q_{\perp 2}^2}}{q_{\perp 1}q_{\perp 2}}. \tag{4.14}$$

This correlation length decreases with rising transverse momenta. Limiting values are

$$L = \begin{cases} \dfrac{b}{\sqrt{2}\,q_{\perp 2}} & \text{for} \quad q_{\perp 1} \gg q_{\perp 2}, \\ \dfrac{b}{\sqrt{2}\,q_{\perp 1}} & \text{for} \quad q_{\perp 2} \gg q_{\perp 1}. \end{cases} \tag{4.15}$$

TABLE I

Comparison of the transverse momentum dependent correlation length $L(q_{\perp 1}, q_{\perp 2})$ according to Eq. (4.14) with data from Ref. [12]. It is $q_{\perp 1} = 2$ GeV/c

$q_{\perp 2}$ (GeV/c)	$L(q_{\perp 1}, q_{\perp 2})$	L_{exp}	Range of experimental $q_{\perp}$ (GeV/c)
0.5	0.52	0.66	0.4 – 0.6
0.7	0.38	0.58	0.6 — 0.8
0.9	0.31	0.50	0.8 – 1.1
1.2	0.24	0.33	1.1 – 1.7

This is just the behaviour found experimentally in the CERN-ISR [12]; see also Figs 5 and 6.

In the Table we compare the correlation lengths obtained from (4.14) with $b = 0.355$ GeV/c with the correlation length which we have determined from the data. We find that Eq. (4.14) reproduces well the trend of the data considering again that the experimental y distribution is probably influenced by the finite acceptance of the trigger particle $\Delta y \simeq 0.1$.

4.3. Rapidity distribution of a second particle from the opposite side jet

The opposite side three-particle distribution considered in Section 3.4, Eq. (3.23), refers to the cross section for a trigger particle 1 from the same side jet and two particles from the opposite side jet. Darriulat et al. [12] found in their experiment some evidence for the opposite side jet by selecting the fastest particle on the opposite side and plotting the distribution of all other opposite side particles over their rapidity separation to the fastest particle. At small rapidity separation to the fastest particle they found a maximum.

Our cross section (3.23) does not correspond exactly to the distribution measured in this experiment; we do not integrate over the transverse momenta of the two opposite side particles and we also have not included the low transverse momentum component. In Fig. 7 we plot rapidity distributions of the second opposite side particle for fixed rapidities and transverse momenta of the trigger particle and the first opposite side particle. In these distributions we find the same behaviour as in the experiment. In respect to their short range correlation two opposite side particles behave similarly as two particles on the same side, and the correlation length $L(q_{\perp 2}, q_{\perp 3})$ of two opposite side particles can be derived from Eq. (3.23) similarly as in Section 4.2 for the same side particles with the same result as there.

5. Summary

In Section 2 we have calculated within a hard collision model the inclusive one-, two-, and three-particle distribution at large transverse momenta taking into account a general jet production function and jet fragmentation with deviation from scaling. The transverse momentum of secondaries within the jet is treated properly. The formalism

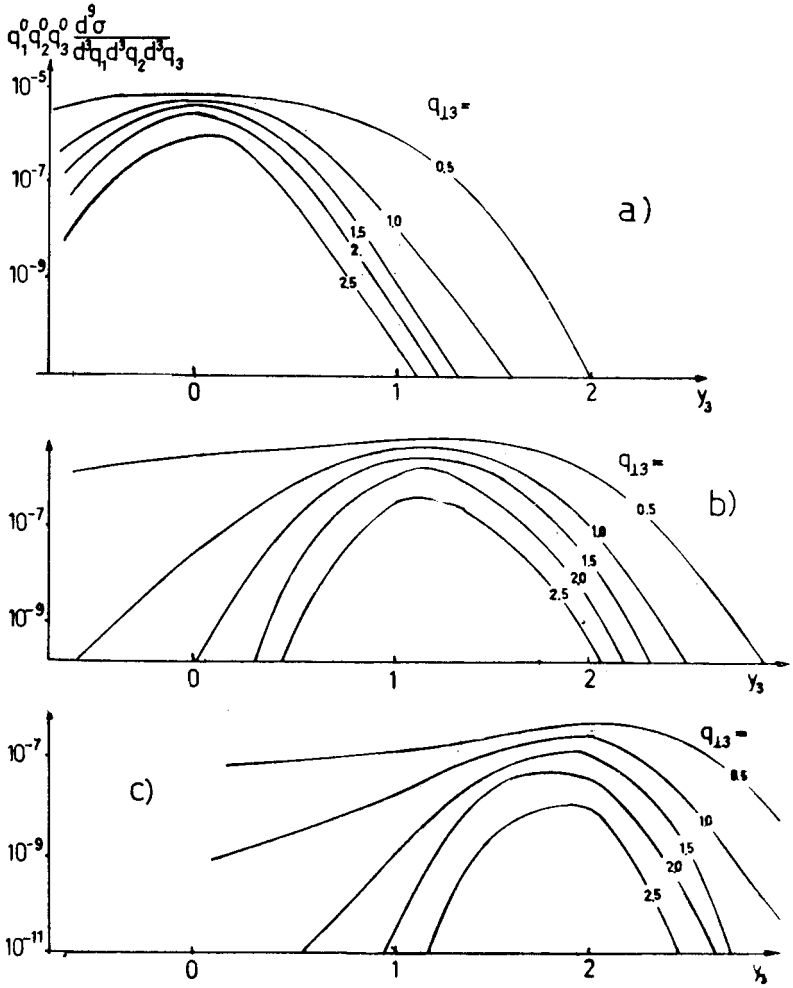

Fig. 7. Opposite side three-particle distribution (particle 1 is the trigger particle; particles 2 and 3 are in the opposite hemisphere) plotted as function of the rapidity of particle 3. The trigger particle has rapidity $y_1 = 0$ and transverse momentum $q_{\perp 1} = 2$ GeV/c. The particle 2 has transverse momentum $q_{\perp 2} = 1.5$ GeV/c and rapidities a) $y_2 = 0$, b) $y_2 = 1$, c) $y_2 = 2$. The transverse momenta of particle 3 are indicated on the curves. Arbitrary units

could be used to study the influence of the jet production dynamics on rapidity and transverse momentum distributions of particles. This is not done here and it seems that more detailed experimental data — in particular regarding the rapidity dependence — would be needed to do this. Using our formalism we study the influence of the transverse momentum dependence within the jet on rapidity correlations between two large transverse momentum particles on the same hemisphere.

We acknowledge discussions with P. V. Landshoff and M. Holder. We thank Mr. Thormann for help with the computer programmes.

REFERENCES

[1] L. DiLella, *Rapporteur talk at the Internat. Symp. on Lepton and Photon Interactions*, Proceedings, Stanford, Ca, Aug. 1975, p.

[2] P. Darriulat, *Rapporteur talk at the Internat. Conf. on High Energy Physics*, Palermo, June 1975.

[3] J. Ranft, G. Ranft, *Nucl. Phys.* **B110**, 493 (1976).

[4] J. D. Bjorken, *Lecture at the SLAC Summer Institute*, July 1975.

[5] S. D. Ellis, M. Jacob, P. V. Landshoff, CERN-preprint TH.

[6] J. D. Bjorken, *Phys. Rev.* **D8**, 4098 (1973).

[7] S. Berman, J. D. Bjorken, J. Kogut, *Phys. Rev.* **D4**, 3388 (1971).

[8] S. D. Ellis, M. B. Kislinger, *Phys. Rev.* **D9**, 2027 (1974).

[9] R. Blankenbecler, S. J. Brodsky, J. F. Gunion, *Phys. Rev.* **D6**, 2652 (1972).

[10] P. V. Landshoff, J. C. Polkinghorne, *Phys. Rev.* **D8**, 4157 (1973).

[11] V. Barger, R. J. N. Phillips, *Nucl. Phys.* **B73**, 269 (1974).

[12] P. Darriulat et al., *Structure of Final States with a High Transverse Momentum π^0 in Proton-Proton Collisions*, preprint, CERN, Febr. 1976.